Phase resetting effects for robust cycles between chaotic sets

Peter Ashwin[a)]
School of Mathematical Sciences, University of Exeter, Exeter EX4 4QE, United Kingdom

Michael Field[b)]
Department of Mathematics, University of Houston, Houston, Texas 77204-3008

Alastair M. Rucklidge[c)] and Rob Sturman[d)]
Department of Applied Mathematics, University of Leeds, Leeds LS2 9JT, United Kingdom

(Received 3 February 2003; accepted 5 May 2003; published 22 August 2003)

In the presence of symmetries or invariant subspaces, attractors in dynamical systems can become very complicated, owing to the interaction with the invariant subspaces. This gives rise to a number of new phenomena, including that of robust attractors showing chaotic itinerancy. At the simplest level this is an attracting heteroclinic cycle between equilibria, but cycles between more general invariant sets are also possible. In this paper we introduce and discuss an instructive example of an ordinary differential equation where one can observe and analyze robust cycling behavior. By design, we can show that there is a robust cycle between invariant sets that may be chaotic saddles (whose internal dynamics correspond to a Rössler system), and/or saddle equilibria. For this model, we distinguish between cycling that includes *phase resetting* connections (where there is only one connecting trajectory) and more general *non(phase) resetting* cases, where there may be an infinite number (even a continuum) of connections. In the nonresetting case there is a question of *connection selection*: which connections are observed for typical attracted trajectories? We discuss the instability of this cycling to resonances of Lyapunov exponents and relate this to a conjecture that phase resetting cycles typically lead to stable periodic orbits at instability, whereas more general cases may give rise to "stuck on" cycling. Finally, we discuss how the presence of positive Lyapunov exponents of the chaotic saddle mean that we need to be very careful in interpreting numerical simulations where the return times become long; this can critically influence the simulation of phase resetting and connection selection. © *2003 American Institute of Physics.* [DOI: 10.1063/1.1586531]

One of the main obstructions to a good understanding of the dynamics of high-dimensional coupled systems (such as neural information processing networks) is the relative absence of a clear and useful classification of the attractors that one can typically find; see Refs. 1, 2. For this reason, the recognition that chaotic itinerancy can occur in such systems is a significant step towards a better classification. Similar behavior, where attractors show robust intermittent behavior has been seen in models with symmetries or invariant subspaces such as Refs. 3, 4; see the review of Krupa.[5] Itinerancy in the form of robust heteroclinic cycles has been found in several models for coupled cells; for example, Refs. 6–8, and there are related weak notions of attraction such as those considered in Refs. 2, 9, 10 as well as cycles between chaotic sets.[11] In this paper we examine a specific ordinary differential equation (ODE) model for a robust cycle between chaotic and equilibrium saddles that is amenable to analysis. For this model we discuss the qualitative properties of phase resetting connections and the selection of connections.

I. INTRODUCTION

There is still much that is not understood about the typical form of robust heteroclinic-like attractors. In this paper, we examine a particular feature (phase resetting) that is not present in connections between equilibria but that is common in cycles between more complicated invariant sets. This type of behavior has been seen in systems of cyclically coupled maps[12,13] and also in a truncated model of magnetoconvection.[14] However, the analysis of the first system requires the inclusion of singularities in the map while the latter system is too complicated to analyze fully. In this paper we consider a new model ODE on $\mathbf{R}^6$ with symmetry $G = (\mathbf{Z}_2)^3$, where a wide variety of attracting robust cycles are possible. Moreover, the ODE is simple enough to be amenable to analysis.

In Sec. II we describe the ODE, which is constructed by coupling a Guckenheimer–Holmes robust heteroclinic cycle[3] with a Rössler system[15] in such a way that the following occurs.

(i) There are attractors that include cycles between saddle equilibria and saddle chaotic sets.
(ii) The attractors persist under perturbations that preserve the symmetry G.

[a)]Electronic mail: P.Ashwin@ex.ac.uk
[b)]Electronic mail: mf@uh.edu
[c)]Electronic mail: A.M.Rucklidge@leeds.ac.uk
[d)]Electronic mail: rsturman@amsta.leeds.ac.uk

(iii) The system is well approximated by a skew product in a neighborhood of each saddle, but globally is not a skew product system.

This model was developed from a skew product system considered previously in Ref. 10. The skew product structure in this system arose through the Rössler system acting as a forcing system on the Guckenheimer–Holmes system. Our new model breaks the skew product to a more general two-way coupling and allows new and, we believe, more typical behavior.

In Sec. III, we show that the model displays a range of cycling chaotic attractors including cycles between equilibria and chaotic saddles. We also describe how these attractors lose stability. We distinguish between *phase resetting* connections, where there is only one connection between two saddles (or "nodes") in the cycle, and *nonresetting* connections with a possibly infinite number of connections (the latter corresponds to the "free running" scenario described in Ref. 12). The system has been constructed to show both types of behavior. We also predict and examine the loss of stability of such robust attracting cycles at resonance bifurcation by using transverse Lyapunov exponents. For the mapping model studied in Ref. 12, phase resetting is associated with the bifurcation of an infinity of stable periodic solutions whereas the nonresetting results in attractors that are chaotic and approximately follow the cycling. For the cycle studied here, one connection is always nonresetting and we observe dynamics exhibiting aspects of both nonphase resetting and phase resetting cycles, but with a complicated detailed structure. We mention some problems that arise in the numerical simulation of this cycle. In particular, we show how phase resetting may be lost due to numerical inaccuracies and we believe this is an issue that needs to be better understood for the simulation of general robust and chaotic itinerant attractors.

In Sec. IV we investigate the classification of more general robust cycling attractors. We highlight the problem of *cycle selection* in nonresetting cycles. Specifically, if there are an infinite number of connections, which of them will appear in the ω-limit set for "typical" initial conditions?

Finally, in Sec. V, we briefly sum up some ideas for extensions of this work.

II. AN ODE MODEL WITH ROBUST CYCLING BETWEEN CHAOTIC SADDLES

Let S^2 denote the unit sphere in $\mathbf{R}^3$. We will define a coupled system of ODEs on $S^2\times\mathbf{R}^3$. The uncoupled dynamics will basically be the product of the Guckenheimer–Holmes dynamics with those of the Rössler equation. Throughout, we denote coordinates on $S^2\times\mathbf{R}^3$ by $(\mathbf{x},\mathbf{y})$, where $\mathbf{x}=(x_1,x_2,x_3)$ and $\Sigma x_i^2=1$.

A. The Guckenheimer–Holmes and Rössler systems

We start by defining a vector field on S^2 that is related to the Guckenheimer–Holmes system. If $Q:\mathbf{R}^3\to\mathbf{R}^3$ is any smooth function and $\langle\cdot,\cdot\rangle$ the standard inner product, we define a smooth vector field F on S^2 by

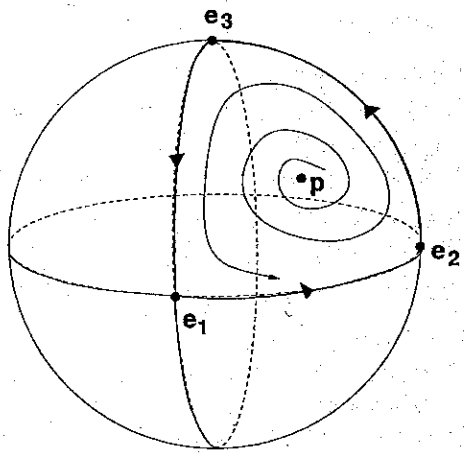

FIG. 1. Guckenheimer–Holmes dynamics on one octant of the sphere for the case $b+c$, bc, $b<0$.

$$F(\mathbf{x})=Q(\mathbf{x})-\langle Q(\mathbf{x}),\mathbf{x}\rangle\mathbf{x},\quad \mathbf{x}\in S^2.$$

Note that if Q is radial (a multiple of $\mathbf{x}$) then $F\equiv 0$. We define a parametrized family $F(\mathbf{x};b,c,d)$ of vector fields on S^2 by taking $Q=(Q_1,Q_2,Q_3)$, where

$$Q_1(\mathbf{x},b,c,d)=x_1(bx_2^2+cx_3^2+dx_2^2x_3^2),$$

$$Q_2(\mathbf{x},b,c,d)=x_2(bx_3^2+cx_1^2+dx_3^2x_1^2),$$

$$Q_3(\mathbf{x},b,c,d)=x_3(bx_1^2+cx_2^2+dx_1^2x_2^2),$$

and b, c, d are real parameters.

The equations used in computational simulations are either obtained by constraining $\dot{\mathbf{x}}=F(\mathbf{x})$ to $\mathbf{x}\in S^2$ or by adding radial dynamics that causes S^2 to become attracting. That is, by considering $\dot{\mathbf{x}}=\tilde{F}(\mathbf{x})$, where

$$\tilde{F}(\mathbf{x})=(1-|\mathbf{x}|^2)\mathbf{x}+F(\mathbf{x}).$$

The models F and $\tilde{F}$ clearly reduce to the same vector field on S^2, and S^2 is flow invariant for the dynamics defined by $\tilde{F}$. In Fig. 1 we show the dynamics on S^2 for the case $d=0$ and $b+c$, bc, $b<0$ [for details and computation, see Field (Ref. 16, Chap. 6)]. Referring to the figure, $\mathbf{e}_1$, $\mathbf{e}_2$, $\mathbf{e}_3$ are the positive unit vectors along the x_1, x_2 and x_3 axes, respectively, and at $\mathbf{p}$. When $bc<0$, the only zeros of F in the first octant of S^2 are $\mathbf{e}_1$, $\mathbf{e}_2$, $\mathbf{e}_3$, and $\mathbf{p}$. The equilibria $\mathbf{e}_1$, $\mathbf{e}_2$, $\mathbf{e}_3$ are hyperbolic saddles. If $b+c<0$, then $\mathbf{p}$ is a source and the saddle connections between $\mathbf{e}_1$, $\mathbf{e}_2$, $\mathbf{e}_3$ form an attracting heteroclinic cycle. Since F is equivariant with respect to the action of G on S^2 defined by $(x_1,x_2,x_3)\mapsto(\pm x_1,\pm x_2,\pm x_3)$, the dynamics in the remaining octants is obtained by repeated reflection in the coordinate planes of the dynamics in the first octant.

Remark 2.1: The great circles on S^2 defined by the intersection of S^2 with the coordinate planes are flow invariant for the dynamics of the vector field F. This invariance is preserved when we couple with the Rössler system and it follows that we shall only need to consider dynamics on the flow invariant first octant of S^2.

On $\mathbf{R}^3$ the Rössler system $\dot{\mathbf{y}}=G(\mathbf{y})$ (with specific parameter choices) is defined by

$$G_1(\mathbf{y})=-y_2-y_3,$$

$$G_2(\mathbf{y}) = y_1 + 0.2y_2,$$

$$G_3(\mathbf{y}) = 0.2 + y_3(y_1 - 5.7),$$

and it is well known (see, for example, Ref. 15) that solutions of this system with initial conditions close enough to the origin are observed to converge to a compact chaotic attractor $\mathcal{A}$. In addition to $\mathcal{A}$, the system has equilibria at

$$\mathbf{y}^A \approx (0.007, -0.035, 0.035),$$

and

$$\mathbf{y}^B \approx (-5.71, 28.54, -28.54).$$

Both equilibria are hyperbolic saddles: $\mathbf{y}^A$ has a one-dimensional stable manifold and a two-dimensional unstable manifold with expanding complex eigenvalues; $\mathbf{y}^B$ has one-dimensional stable and two-dimensional unstable manifolds with real eigenvalues. However, the second equilibrium will not be of particular interest for the parameter values considered in this paper.

B. Definition of the coupled system

We define a smooth map $\mu: S^2 \to \mathbf{R}$ by

$$\mu(\mathbf{x}) = \frac{\tanh(4(2x_1^2 - 1)) + \tanh(4)}{2\tanh(4)}.$$

The function μ is chosen so that $\mu(0)=0$, μ is even in x_1, and $\mu(\pm 1)=1$. Moreover, μ increases monotonically with the greatest rate of change occurring near the circles $x_1 = \pm\frac{1}{2}$ on the unit sphere.

For $\epsilon > 0$, let Δ_ϵ denote the diagonal matrix $\mathrm{diag}(\epsilon, 2\epsilon, 3\epsilon)$ and pick a fixed vector $\mathbf{y}^F = (y_1^F, y_2^F, y_3^F) \in \mathbf{R}^3$. The dynamics of the $\mathbf{y}$ variables will be coupled to the $\mathbf{x}$ variables by the $\mathbf{x}$-dependent term $-\mu(\mathbf{x})\Delta_\epsilon(\mathbf{y} - \mathbf{y}^F)$. We also couple the $\mathbf{x}$ dynamics to the $\mathbf{y}$ dynamics by making the coefficients b and c functions of $\mathbf{y}$.

We define our coupled system of ODEs on $S^2 \times \mathbf{R}^3$ by

$$\begin{aligned} \dot{\mathbf{x}} &= F(\mathbf{x}; b(\mathbf{y}), c(\mathbf{y}), d), \\ \dot{\mathbf{y}} &= (1 - \mu(\mathbf{x}))G(\mathbf{y}) - \mu(\mathbf{x})\Delta_\epsilon(\mathbf{y} - \mathbf{y}^F), \end{aligned} \tag{1}$$

where

$$b(\mathbf{y}) = b_0 + b_1 \sin(y_1), \quad c(\mathbf{y}) = c_0 + c_1 \sin(y_3).$$

Observe that when $\mu = 0$ (and $x_1 = 0$, $x_2^2 + x_3^2 = 1$), the $\mathbf{y}$ dynamics are identical to the Rössler equations, whereas for $\mu = 1$ ($x_1 = \pm 1$, $x_2 = x_3 = 0$), $\mathbf{y}$ has an attracting fixed point at $\mathbf{y}^F$.

The group $(\mathbf{Z}_2)^3$ of reflections on S^2 extends to the action on $S^2 \times \mathbf{R}^3$, defined by

$$(x_1, x_2, x_3, y_1, y_2, y_3) \mapsto (\pm x_1, \pm x_2, \pm x_3, y_1, y_2, y_3).$$

Since μ is clearly $(\mathbf{Z}_2)^3$ invariant, it follows that for any choice of parameters, the system (1) is symmetric with respect to $(\mathbf{Z}_2)^3$.

Remark 2.2: The Guckenheimer–Holmes[3] model is also symmetric with respect to the $\mathbf{Z}_3$ action defined by $(x_1, x_2, x_3) \mapsto (x_2, x_3, x_1)$. However, μ is not $\mathbf{Z}_3$ invariant and so (1) is *not* $\mathbf{Z}_3$ symmetric. Indeed, we have deliberately broken the $\mathbf{Z}_3$ symmetry to ensure that we can obtain cycles between saddles with different dynamics. However, it is easy to verify that the subspace $\{\mathbf{p}\} \times \mathbf{R}^3$ *is* flow invariant for the system (1). Solutions lying on this subspace can be regarded as *synchronized* solutions. These solutions will not play a major role for us in this paper.

TABLE I. With the exception of M, the listed subspaces of $S^2 \times \mathbf{R}^3$ (or $\mathbf{F}$) are invariant for any $(\mathbf{Z}_2)^3$-symmetric flow on $S^2 \times \mathbf{R}^3$. The second column gives the notation we use for the intersection of this space with $\mathbf{F}$.

Name	Intersection with $\mathbf{F}$	Subspace	Dim
$\pm P_1$	P_1	$\{\pm \mathbf{e}_1\} \times \mathbf{R}^3$	3
$\pm P_2$	P_2	$\{\pm \mathbf{e}_2\} \times \mathbf{R}^3$	3
$\pm P_3$	P_3	$\{\pm \mathbf{e}_3\} \times \mathbf{R}^3$	3
M	$\mathbf{p}$	$\{\mathbf{p}\} \times \mathbf{R}^3$	3
N_{12}	E_{12}	$S_{12} \times \mathbf{R}^3$	4
N_{23}	E_{23}	$S_{23} \times \mathbf{R}^3$	4
N_{13}	E_{13}	$S_{13} \times \mathbf{R}^3$	4

For $i < j \in \{1,2,3\}$, let S_{ij} denote the great circle of S^2 defined as the intersection of the $x_i x_j$-coordinate plane with S^2. Each S_{ij} is flow invariant for every $(\mathbf{Z}_2)^3$ symmetric flow on S^2. The pairwise intersections of all the circles S_{ij} define the points $\pm \mathbf{e}_k$, $k = 1,2,3$, which must be flow invariant, and therefore equilibria, for every $(\mathbf{Z}_2)^3$ symmetric flow on S^2. Let $\mathbf{O} = \{\mathbf{x}: x_1 \geq 0, x_2 \geq 0 \text{ and } x_3 \geq 0\}$ denote the positive octant of S^2. Set

$$\mathbf{F} = \mathbf{O} \times \mathbf{R}^3 \subset S^2 \times \mathbf{R}^3,$$

and let E_{ij} denote the flow invariant subsets of $S^2 \times \mathbf{R}^3$ defined by the intersection of $S_{ij} \times \mathbf{R}^3$ with $\mathbf{F}$.

In Table I we list the subspaces of $S^2 \times \mathbf{R}^3$ and $\mathbf{F}$ that are flow invariant for (1). These are depicted schematically in Fig. 2.

It follows from Table I that $\partial\mathbf{F} = \cup_{i,j} E_{ij}$ is flow invariant and so $\mathbf{F}$ is a flow-invariant subspace of $S^2 \times \mathbf{R}^3$. Moreover, just as for the Guckenheimer–Holmes system, once we can describe the flow on $\mathbf{F}$ we can obtain the rest of the flow on $S^2 \times \mathbf{R}^3$ by applying symmetry transformations [$\mathbf{F}$ is a *fundamental domain* for the action of $(\mathbf{Z}_2)^3$ on $S^2 \times \mathbf{R}^3$]. Henceforth in this paper we will restrict attention to the flow of (1) on $\mathbf{F}$.

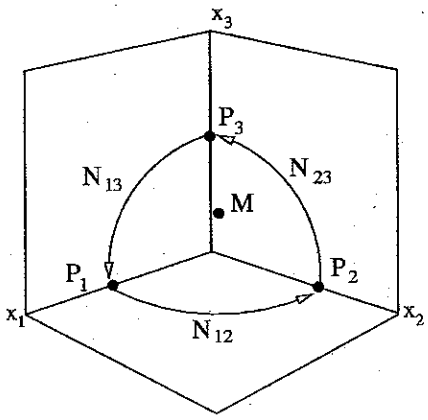

FIG. 2. A schematic representation of the invariant subspaces for the system (1) projected onto the x_i coordinates. There can be robust connections between invariant sets in the P_i with connections in the illustrated invariant subspaces N_{ij}.

The dynamics of the $\mathbf{y}$ variables in the system can be characterized as follows. On the subspace E_{23} of $\mathbf{F}$ defined by $x_1=0$, the dynamics are those of the Rössler equation and so trajectories starting close enough to the origin will typically be asymptotic to a Rössler attractor $\mathcal{A}$. On the other hand, when $x_1=1$ (and $x_2=x_3=0$), then the dynamics on P_1 will be asymptotic to the globally attracting fixed point $\mathbf{y}^F$ with eigenvalues $-\epsilon$, -2ϵ, -3ϵ. Roughly speaking, for initial conditions $\mathbf{x}_0$ between these states, trajectories projected into $\mathbf{R}^3$ ($\mathbf{y}$ space) switch between these extreme states. For future reference, we define

$$\mathcal{A}_j=\{\mathbf{e}_j\}\times\mathcal{A}\subset P_j,$$

for $j=2,3$. The sets $\mathcal{A}_j$ are Rössler attractors for the flow of (1) restricted to P_j, $j=2,3$.

C. Equilibria for the coupled system

The system (1) has five hyperbolic equilibria in the flow-invariant set $P_1\cup P_2\cup P_3$. We shall be interested in three of these equilibria:

$$\mathbf{q}_1=(\mathbf{e}_1,\mathbf{y}^F),\quad \mathbf{q}_2=(\mathbf{e}_2,\mathbf{y}^A),\quad \text{and}\quad \mathbf{q}_3=(\mathbf{e}_3,\mathbf{y}^A).$$

[The other two equilibria are $(\mathbf{e}_2,\mathbf{y}^B)$ and $(\mathbf{e}_3,\mathbf{y}^B)$.]

The issue of whether or not there exist any other equilibria in $\partial\mathbf{F}$ for (1) is trickier and we sketch only some partial results. Let e_{ij} denote the edge $S_{ij}\cap\mathbf{O}$, $i<j\in\{1,2,3\}$. If $(\mathbf{x},\mathbf{y})\in\partial\mathbf{F}$ is a hyperbolic equilibrium with $\mathbf{x}$ interior to the edge e_{ij}, then we must have

$$(b_0+b_1\sin y_1)(c_0+c_1\sin y_3)>0. \tag{2}$$

If we replace $\mu(\mathbf{x})$ in (1) by the new variable $a\in(0,1)$, we find two equilibrium points $\mathbf{u}(a)$, $\mathbf{v}(a)$ for $\mathbf{y}$. These can determine equilibrium points of (1) only if (2) is satisfied. For example, if $|b_0|>|b_1|$, $|c_0|>|c_1|$ and $b_0c_0<0$ then we can never satisfy (2) and so in this case there must be exactly five equilibrium points in $\partial\mathbf{F}$.

If U is an open isolating neighborhood of the Rössler attractor $\mathcal{A}\subset\mathbf{R}^3$ and $b(\mathbf{y})c(\mathbf{y})<0$, all $\mathbf{y}\in U$, then there will be no equilibria of (1) in $e_{23}\times U\subset E_{23}$. This implies that all trajectories in interior(E_{23}) with initial conditions close enough to $\mathcal{A}_2\subset P_2$ will be forward asymptotic to $\mathcal{A}_3\subset P_3$. Rather than this strong assumption, we will instead choose parameter values (see Sec. III) such that the *ergodic average* of $b(\mathbf{y})c(\mathbf{y})$ over $\mathcal{A}$ is negative.

Matters are more difficult when we study the dynamics on interior(E_{12}) and interior(E_{31}). One way of proceeding is to replace the smooth function μ with a discontinuous threshold function, say

$$\bar{\mu}(\mathbf{x})=0,\quad |x_1|<\tfrac{1}{2},$$
$$=1,\quad |x_1|\geqslant\tfrac{1}{2}.$$

The advantage of using a function of this form is that it now becomes relatively easy to obtain precise analytical estimates (see Ref. 16). The disadvantage is that it becomes much harder to estimate errors in numerical investigations. In any case, if we assume that (1) $b(\mathbf{y})c(\mathbf{y})<0$, all $\mathbf{y}\in U$, where U is an isolating neighborhood of $\mathcal{A}$, and (2) $\mathbf{y}^F\in U$, then it is possible to verify that in this case there are no new equilibria in $\partial\mathcal{O}\times U$ and that every trajectory starting in $\partial\mathcal{O}\times U$ stays in $\partial\mathcal{O}\times U$ and is forward asymptotic to either $\mathbf{y}^F$ or one of $\mathcal{A}_2$, $\mathcal{A}_3$. This result continues to hold if we approximate $\bar{\mu}$ by a smooth function equal to $\bar{\mu}$ away from a small neighborhood of $|x_1|=1/2$.

D. Stabilities of the equilibria forced by symmetry

Given any $\mathbf{y}\in\mathbf{R}^3$, we define

$$\eta(\mathbf{y})=(b_0+b_1\sin y_1)(c_0+c_1\sin y_3)=b(\mathbf{y})c(\mathbf{y}).$$

Since we are interested in cycles, we consider only the case in which $\eta(\mathbf{y}^F)<0$, $\eta(\mathbf{y}^A)<0$. This guarantees that each of these equilibria has one expanding and one contracting eigendirection on S^2. Note that though this is not a sufficient condition for the existence of a cycle, it does enable us to compute the dimensions of the stable and unstable manifolds of the equilibria. Furthermore, we restrict to the case $b(\mathbf{y}^F)<0$, $b(\mathbf{y}^A)<0$, so that the orientation of a cycle has to be $\mathbf{e}_1\to\mathbf{e}_2\to\mathbf{e}_3\to\mathbf{e}_1$. Since $\mathbf{y}^A$ is a fixed point of the Rössler system, and since $\mathbf{y}^F$ is an $\mathbf{x}$-independent equilibrium of $(\mathbf{y}-\mathbf{y}^F)$, the subspaces $(\mathbf{e}_1,\mathbf{y}^F)$, $(\mathbf{e}_2,\mathbf{y}^A)$, $(\mathbf{e}_3,\mathbf{y}^A)$, and $e_{23}\times\{\mathbf{y}^A\}$ are invariant. If $\mathbf{y}^F=\mathbf{y}^A$, all the subspaces $(\mathbf{e}_i,\mathbf{y}^F)$ and $e_{ij}\times\{\mathbf{y}^F\}$ are invariant.

If we regard S^2 as embedded in $\mathbf{R}^3$ and compute the Jacobian in $\mathbf{R}^3\times\mathbf{R}^3$, we find, for example, that

$$J(\mathbf{q}_2)=\begin{pmatrix} b_0+b_1\sin y_1^A & 0 & 0 & 0\\ 0 & 0 & 0 & 0\\ 0 & 0 & c_0+c_1\sin y_3^A & 0\\ 0 & 0 & 0 & E(\mathbf{y}^A)\end{pmatrix},$$

where $E(\mathbf{y})$ is the Jacobian of the Rössler equation at $\mathbf{y}$. The row of zeros follows since S^2 is flow invariant for (1) and the (normal or radial) $\partial/\partial x_j$ derivative is zero at $\mathbf{e}_2$. [For $\tilde{F}$ we have a -2 eigenvalue since S^2 is flow invariant and globally attracting for (1). The radial direction is disregarded in the following discussion of dimensions.] The block diagonal structure of the matrix gives the dimensions of stable and unstable manifolds of the equilibria directly. Hence the eigenvalues of the Jacobian of (1) at $\mathbf{q}_2$ are $b_0+b_1\sin y_1^A$, $c_0+c_1\sin y_3^A$, together with three eigenvalues for Rössler equations at $\mathbf{y}^A$ [recall that $E(\mathbf{y}^A)$ has one negative eigenvalue and two eigenvalues with a positive real part]. Thus, the points $\mathbf{q}_j$, $j=2,3$, have a three-dimensional unstable manifold consisting of the two unstable directions leading to $\mathcal{A}_j$ and the unstable direction normal to P_j. Evaluating the Jacobian at the point $\mathbf{q}_1$ similarly gives a diagonal matrix with entries $b_0+b_1\sin y_1^F$, 0, $c_0+c_1\sin y_3^F$, $-\epsilon$, -2ϵ, -3ϵ. Hence, the point $\mathbf{q}_1$ has a one-dimensional unstable manifold.

In the following we will assume that $\mathbf{y}^F$ is close to $\mathbf{y}^A$. It is important to note that if $\mathbf{y}^F=\mathbf{y}^A$, then the unstable manifold of $\mathbf{q}_1$ cannot be transverse to the stable manifold of $\mathbf{q}_2$. Indeed, if $\mathbf{y}^F=\mathbf{y}^A$, then the unstable manifold of $\mathbf{q}_1$ (in $\mathbf{F}$) is $e_{12}\times\{\mathbf{y}^F\}$ [less the point $\mathbf{q}_2=(\mathbf{e}_2,\mathbf{y}^F)$] and is therefore *con-*

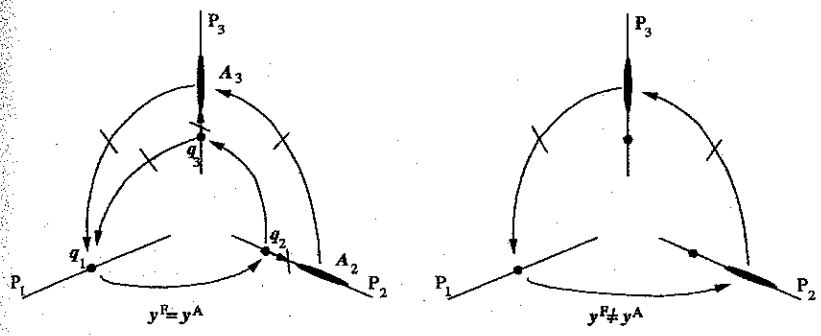

FIG. 3. The dynamics on $\partial\mathbf{F}$ for $\mathbf{y}^F=\mathbf{y}^A$, and the more general case $\mathbf{y}^F$ not equal but close to $\mathbf{y}^A$. The connections that are crossed consist of an infinite number of connections, while those that are not crossed are phase resetting. For $\mathbf{y}^A=\mathbf{y}^F$, the connection in E_{12} occurs between equilibria; otherwise it is from equilibrium to chaotic saddle.

tained in the stable manifold of $\mathbf{q}_2$. When $\mathbf{y}^F\neq\mathbf{y}^A$, the unstable manifold of $\mathbf{q}_1$ does not intersect the stable manifold of $\mathbf{q}_2$.

We sum up our computations and observations in the next lemma and Fig. 3. The connections between sets are verified numerically in the next section.

Lemma 2.3: There is a nonempty open set of parameters b_0, b_1, c_0, c_1, d, ϵ *and* $\mathbf{y}^F$ *such that*

$$\dim(W^u(\mathbf{q}_1))=1,$$

and

$$\dim(W^u(\mathbf{q}_2))=\dim(W^u(\mathbf{q}_3))=3.$$

If we assume that

$$W^u(\mathcal{A}_2)\subset W^s(\mathcal{A}_3),\quad W^u(\mathcal{A}_3)\subset W^s(\mathbf{q}_1),$$

and

$$W^u(\mathbf{q}_1)\subset W^s(\mathbf{q}_2\cup\mathcal{A}_2),\quad W^u(\mathbf{q}_2)\subset W^s(\mathcal{A}_2\cup\mathbf{q}_3\cup\mathcal{A}_3),$$

$$W^u(\mathbf{q}_3)\subset W^s(\mathcal{A}_3\cup\mathbf{q}_1).$$

Then

$$W^u(\mathbf{q}_1)\subset\begin{cases}W^s(\mathbf{q}_2), & \text{for } \mathbf{y}^F=\mathbf{y}^A,\\ W^s(\mathbf{A}_2), & \text{for } \mathbf{y}^F\neq\mathbf{y}^A,\end{cases}$$

and the system has heteroclinic networks as illustrated in Fig. 3.

Our system has a total of nine real parameters: b_0, b_1, c_0, c_1, d, ϵ, and $\mathbf{y}^F$. The cycles shown in Fig. 3 are only robust for the case $\mathbf{y}^F\neq\mathbf{y}^A$; and then they will be present for a nonempty open set of parameter values. In the next section we examine the stability of the cycles.

Referring to the figure, we remark that P_1 contains the equilibrium point $\mathbf{q}_1$ that is attracting within P_1. The invariant subspaces P_2 and P_3 contain the saddle points $\mathbf{q}_j$, $j=2,3$, as well as copies of the Rössler attractor $\mathcal{A}$. Stabilities of the saddle points in $\partial\mathbf{F}$ are as indicated in Fig. 3. The saddle points $\mathbf{q}_j$, $j=2,3$ have invariant manifolds contained within $\partial\mathbf{F}$ and $\dim(W^u(\mathbf{q}_j))=3$, $\dim(W^s(\mathbf{q}_j))=2$ in both cases. Since $\mu\equiv 0$ on E_{23}, it follows easily from the explicit equations that $W^u(\mathbf{q}_2)$ intersects $W^s(\mathbf{q}_3)$ transversally along the connection $e_{23}\times\{\mathbf{y}^A\}$. Generically, we expect that $W^u(\mathbf{q}_2)$ meets $W^s(\mathbf{q}_3)$ transversally within all of E_{23}, in which case there exist finitely many connections from $\mathbf{q}_2$ to $\mathbf{q}_3$. Although, in principle, there can exist more than one connection from $\mathbf{q}_2$ to $\mathbf{q}_3$, we mark the connection $\mathbf{q}_2\to\mathbf{q}_3$ as phase resetting.

III. ATTRACTORS INVOLVING CYCLING FOR THE MODEL

Robust homoclinic cycles between invariant sets can gain or lose stability at a *resonance bifurcation*—that is, for parameter values at which the expanding and contracting eigenvalues become equal in magnitude.[17] A similar mechanism, using Lyapunov exponents in place of eigenvalues, can cause cycles between chaotic saddles to gain and lose stability; see, for example, Refs. 10, 14. The presence in (1) of invariant subspaces greatly simplifies the calculation of the normal Lyapunov exponents. The cycle in question is between three invariant subspaces—one containing an equilibrium, and two containing chaotic saddles, respectively, $\mathbf{q}_1$, $\mathcal{A}_2$, and $\mathcal{A}_3$. To calculate the normal Lyapunov exponents of the cycle we multiply together the normal Lyapunov exponents of the constituent parts of the cycle. As earlier, the block diagonal structure of the Jacobian makes it very simple to calculate these exponents. In particular, the contracting and expanding normal Lyapunov exponents at $\mathbf{q}_1$, which we call $\lambda_c^{(\mathbf{q}_1)}$ and $\lambda_e^{(\mathbf{q}_1)}$, respectively, are given by $\lambda_c^{(\mathbf{q}_1)}=b_0+b_1\sin y_1^F$ and $\lambda_e^{(\mathbf{q}_1)}=c_0+c_1\sin y_3^F$. The normal exponents at $\mathcal{A}_2$ and $\mathcal{A}_3$ can also be found (see Ref. 10) by averaging the derivatives. Hence for an ergodic invariant measure supported on $\mathcal{A}_2$ the transverse Lyapunov exponents are

$$\lambda_c^{(\mathcal{A}_2)}(\mu)=\int_{\mathcal{A}_2} b(u,v,w)\,d\mu(u,v,w),$$

$$\lambda_e^{(\mathcal{A}_2)}(\mu)=\int_{\mathcal{A}_2} c(u,v,w)\,d\mu(u,v,w),$$

and similarly for $\mathcal{A}_3$. These can be approximated as in Ref. 10 to give

$$(\lambda_c^{(\mathcal{A}_2)},\lambda_e^{(\mathcal{A}_2)})=(\lambda_c^{(\mathcal{A}_3)},\lambda_e^{(\mathcal{A}_3)})$$
$$=(b_0-0.053\,60b_1,c_0+0.116\,29c_1).$$

If we define

$$\rho:=\left|\frac{\lambda_c^{(\mathbf{q}_1)}\lambda_c^{(\mathcal{A}_2)}\lambda_c^{(\mathcal{A}_3)}}{\lambda_e^{(\mathbf{q}_1)}\lambda_e^{(\mathcal{A}_2)}\lambda_e^{(\mathcal{A}_3)}}\right|,$$

then we expect the cycle to be asymptotically stable for $\rho>1$ (since in this case the normal contraction onto the cycle dominates over the expansion), and unstable for $\rho<1$. The resonance of Lyapunov exponents occurs at $\rho=1$. We use c_0 as a control parameter to govern the stability of the cycle.

Fixing b_0, b_1, c_1, the resonance condition gives a cubic equation for c_0^* (the value of c_0 at resonance). In all of the following numerics we set $b_0=-0.1$, $b_1=c_1=0.5$, so that the resonance condition becomes

$$644.604(c_0^*+0.017\,56)(c_0^*+0.058\,14)^2=1,$$

which gives $c_0^*=0.072\,85$. Note that for these parameters, we have $\eta(\mathbf{y})<0$ for ergodic trajectories within $\mathcal{A}_2$. We also fix $d=-0.1$, $\epsilon=1$ throughout the following.

It is natural to ask what type of attractors are created when cycling chaos loses stability (or, equivalently, to describe the mechanisms involved in the creation of cycling chaos). These matters have been addressed in Refs. 12–14, with particular reference to the difference between phase resetting effects. A phase resetting connection occurs when there is only one trajectory between two invariant sets. In contrast, for nonresetting connections, an infinite number of different connecting trajectories may be present.

These computations assume that we are in the case $\mathbf{y}^F \neq \mathbf{y}^A$. Observe, moreover, that the connection from $\mathcal{A}_2$ to $\mathcal{A}_3$ is always nonresetting. In the other case $\mathbf{y}^A=\mathbf{y}^F$ the stability of the cycle may also depend on eigenvalues at $\mathbf{q}_2$ and $\mathbf{q}_3$. Previous papers[12–14] have conjectured that phase resetting connections usually give rise to stable periodic orbits whose periods accumulate at a resonance, whereas nonphase resetting connections may not. For the cycles discussed in this paper where some connections may be phase resetting and others are not, we find trajectories that are representative of both types of behavior, but whose detailed structure is a complicated combination.

A. Some numerical results

An accurate simulation of (1) requires some care. As an attracting cycle approaches the invariant subspaces, some of the $\mathbf{x}$ variables get extremely close to zero, while the $\mathbf{y}$ variables remain $O(1)$. These hugely differing scales result in the potential for phenomena that are purely numerical artifacts and some problems caused by this are addressed in more detail in Sec. III B. Figure 4 shows convergence toward a cycling chaotic attractor for $c_0=0.07$, and $\mathbf{y}^F=(0.01,1,0.01)$. The same trajectory is shown in Fig. 5 in logarithmic x coordinates. For these parameter values, the saddle point $\mathbf{q}_1$ has one positive eigenvalue for the Jacobian, and so the connection from $\mathbf{q}_1 \to \mathcal{A}_2$ is phase resetting. The successive approaches to the connections are shown in Fig. 6. Plot (a) shows that the connection $\mathbf{q}_1 \to \mathcal{A}_2$ is phase resetting while the connection $\mathcal{A}_2 \to \mathcal{A}_3$ shown in (b) is nonresetting (see also Fig. 9 later). In Fig. 6 the connection $\mathbf{q}_1 \to \mathbf{q}_2$ is shown in the case $c_0=0.07$ and $\mathbf{y}^F=\mathbf{y}^A$. Numerical errors in the specification of $\mathbf{y}^F$, however, mean that the connection from $\mathbf{q}_1$ to $\mathbf{q}_2$ is not exact and, in fact, we see the same effect as a phase resetting connection (a), just with a long time of residence near $\mathbf{q}_2$ (shown by $y_2=0$ in this plot); we expect great sensitivity to noise in this case.

Each time around the cycle the dynamics get closer to the invariant subspaces E_{ij}, and this is reflected in the approximately geometric increase of the length T_n of the nth epoch (see, for example, Ref. 13). Also plotted is y_2, depicting the change in behavior of the $\mathbf{y}$ variables, as these switch between the fixed point at $\mathbf{q}_1$ and the chaotic behavior of $\mathcal{A}_j$ for $j=2,3$. On increasing c by a small amount we lose attraction of the cycle at a resonance, and for this system, with $d<0$, we appear to create an approximately periodic chaotic attractor—see the example illustrated in Fig. 7 with $c_0=0.09$.

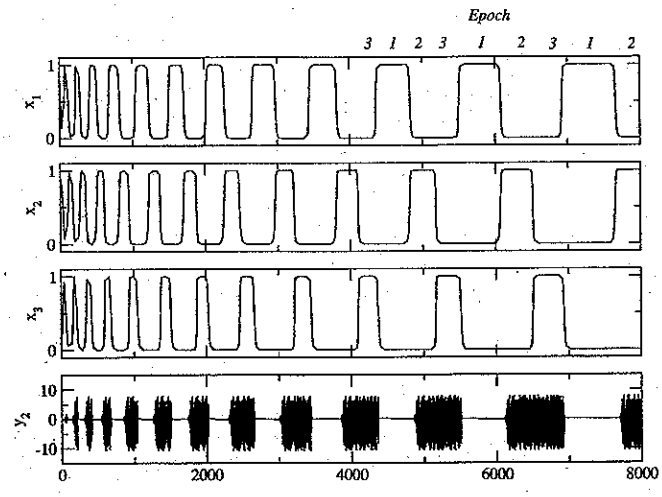

FIG. 4. A trajectory approaching a cycling chaotic attractor for $b_0=-0.1$, $b_1=0.5$, $c_0=0.07$, $c_1=0.5$, $d=-0.1$, $\epsilon=1$, and $\mathbf{y}^F=(0.01,1,0.01)$; time series for three components of x and y_2 are shown. Successive epochs where the trajectory is close to the saddle equilibrium $\mathbf{q}_1$ and the chaotic saddles $\mathcal{A}_2$, $\mathcal{A}_3$ are labeled at the top of the diagram. The connection $\mathbf{q}_1 \to \mathcal{A}_2$ is phase resetting as it follows the one-dimensional unstable manifold for the equilibrium $\mathbf{q}_1$.

Examining the geometric rate of increase R as approximated by $R=T_{n+1}/T_n$ can clarify the behavior for parameters on either side of the resonance bifurcation. Figure 8 shows this ratio plotted against the number of circumnavigations of the cycle for two different parameter values on either side of the resonance. In both plots, the solid line corresponds to $\mathbf{y}^F=(0.01,-0.04,0.04)$ and the dotted line to $\mathbf{y}^F=\mathbf{y}^A\approx(0.007,-0.035,0.035)$ given to within double precision accuracy. In plot (a) we have $c_0=0.08>c_0^*$. We observe that T_{n+1}/T_n tends to unity on a periodic orbit for $\mathbf{y}^F \neq \mathbf{y}^A$. In contrast, for $\mathbf{y}^F=\mathbf{y}^A$ (dotted line) we find instead

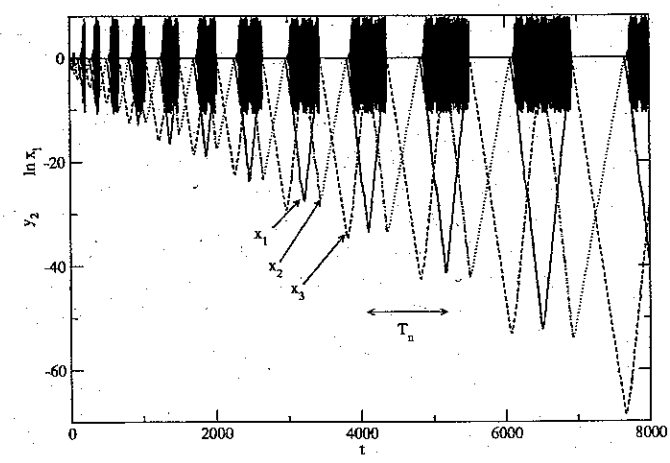

FIG. 5. Attracting cycling chaos shown for the same trajectory as Fig. 4, but instead showing y_2 and the logarithms of the x_i. The lengths of the phases T_n increase approximately geometrically as the trajectory approaches the cycle.

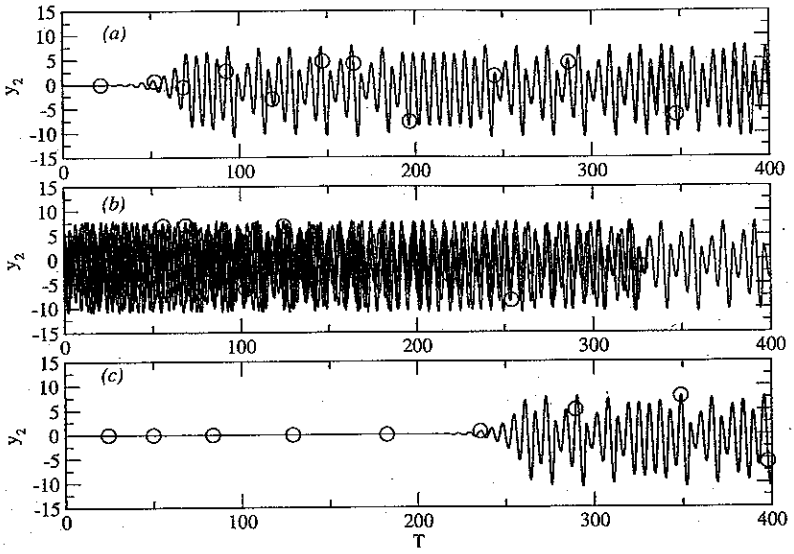

FIG. 6. A number of orbit segments (of increasing length) are shown for (a) a phase resetting connection for the attractor of the trajectory in Fig. 4. Each time the trajectory enters $|x_2|>0.8$ we set T to 0 and each time it leaves $|x_2|>0.8$ we mark by a circle. (b) This shows the nonresetting connection between the chaotic saddles $\mathcal{A}_2$ and $\mathcal{A}_3$ for the same cycle. On entering $|x_3|>0.8$ we set T to 0 and mark with a circle when we leave $|x_3|>0.8$. The segments get longer each time around the cycle as the trajectory slows down, finally leaving a single signal for $T>330$. Observe that there is no apparent coherence comparable to (a). (c) This shows a connection for the case as above, but with $c_0=0.07$ and $\mathbf{y}^F=\mathbf{y}^A$ to double precision accuracy, with $T=0$ on entering $|x_2|>0.8$. Observe that after about 200 time units, numerical inaccuracies in specifying $\mathbf{y}^F$ cause the connection to head toward $\mathcal{A}_2$ as a phase resetting connection.

fluctuations about unity. Here R has a mean of 1.008 with a standard deviation of ± 0.0332. In (b), which has $c_0=0.072<c_0^*$, we expect to find (for both values of $\mathbf{y}^F$) the ratio R tending to a value greater than one, which gives the exponent of the geometric rate of slowing. Both models clearly have T_{n+1}/T_n consistently greater than one, but neither has converged after 80 times around the cycle (the phase resetting system has $R=1.024\pm 0.0258$, and the nonresetting version has $R=1.040\pm 0.0327$). This is symptomatic of the difficulty of numerics for cycles—here the rate of convergence is very slow. We can increase this rate of convergence (and increase R) simply by decreasing c_0, but this also has the effect of making the dynamics approach E_{ij} much more quickly, and so fewer circuits around the cycle are possible before the calculations lose significance.

B. Aspects of numerical simulation

The numerical simulation of approach of trajectories to a cycling attractor, and, in particular, the selection of connection, is difficult to realize accurately because:

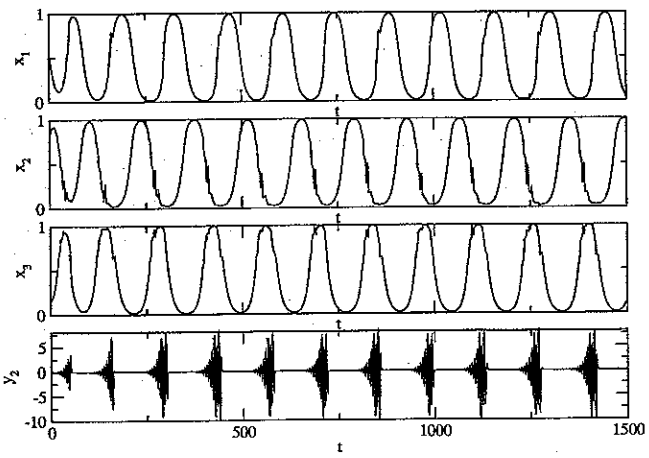

FIG. 7. A trajectory approaching an approximately periodic chaotic attractor for the same parameters as Figs. 4 and 5, but with $c_0=0.09$; time series for three components of x and y_2 are shown. The orbit includes segments of the one-dimensional unstable manifold for the equilibrium $\mathbf{q}_1$.

(1) There are directions with positive Lyapunov exponents within the chaotic saddles $\mathcal{A}_{2,3}$.
(2) The connection selected depends critically on the time of residence near a saddle, and this can become unbounded.

This means that we can only believe the qualitative behavior of connection selection for residence times near saddles that are up to length T such that

$$\eta \exp(\lambda T) \ll 1,$$

where λ is the most positive tangential Lyapunov exponent for the chaotic saddle and η is the machine accuracy. This means that we have an effective time horizon,

$$T < -\frac{\log(\eta)}{\lambda},$$

beyond which errors will have accumulated to the extent that different selection behavior may appear. For the numerics in

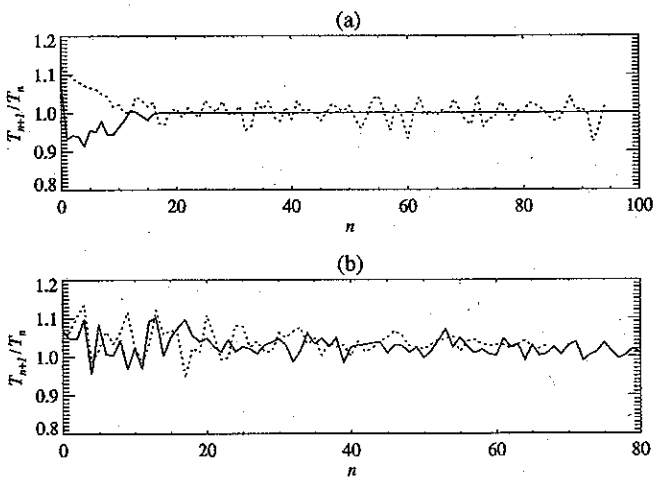

FIG. 8. The ratio R of successive times T_n plotted against circumnavigations n. The fixed parameters are (as before) $b_0=-0.1$, $b_1=-0.5$, $c_1=0.5$, $d=-0.1$, $\epsilon=1$. Solid lines represent the phase resetting model with $\mathbf{y}^F=(0.01,-0.04,0.04)$ and dotted lines the nonresetting version with $\mathbf{y}^F=\mathbf{y}^A$ (to double precision accuracy). The control parameter values are (a) $c_0=0.08>c_0^*$; (b) $c_0=0.072<c_0^*$.

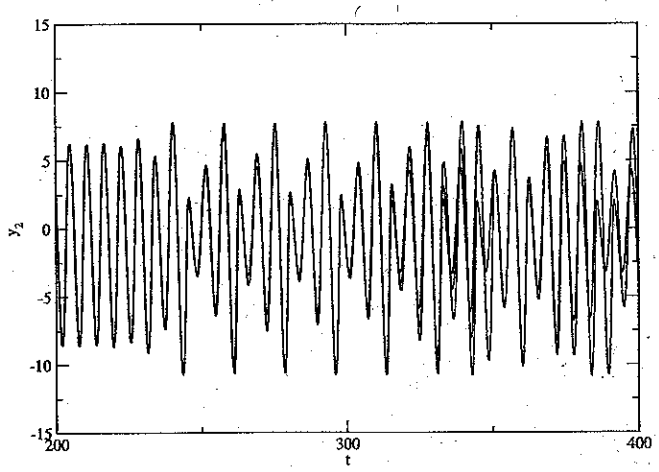

FIG. 9. Loss of coherence after a phase resetting connection during attracting cycling. After approximately 300 time units for the trajectory segments shown in Fig. 6(a) one loses coherence due to numerical inaccuracy.

Sec. III A we can estimate λ as approximately 0.0713 for the Rössler system. Hence, for order one $\mathbf{y}$ at double-precision accuracy, we have $\eta = 10^{-16}$ and can expect separation from a phase resetting connection after a few hundred time units. Figure 9 illustrates this effect.

Even for cycles that are shorter than this, computation of Lyapunov exponents has to be done very carefully due to the fact that the local behavior changes greatly as one moves around the cycle. Therefore, any Lyapunov exponent calculation will typically show very large fluctuations and slow convergence as the trajectory proceeds around the cycle.

A similar effect in the computation of approaches to invariant subspaces is observed in Refs. 14, 18, which can be overcome by representing the distance from the invariant subspace using an exponential numerical grid. This approach is not easily transferable to the sort of problem we consider here, as the distance from a given *trajectory* $W^u(\mathbf{q}_1)$ (rather than from a single point) would need to be stored in an exponential grid.

Finally, we remark that we can change the choice of the numerical value 4 in the definition of the function μ so as to vary $\max \mu'$. However, that if $\max \mu'$ becomes too large, this can cause problems for the numerical integration. On the other hand, if $\max \mu'$ is too small then the coupling can create new invariant sets near those in which we are interested, and further complicate the dynamics.

IV. CONNECTION SELECTION FOR NONRESETTING CYCLES

The attractors we observe in the model (1) are comprised of a finite number of *nodes*—saddle equilibria or chaotic saddles—together with possibly infinitely many *connections*.

In what follows, we continue to work within the fundamental domain $\mathbf{F}$. Let ϕ_t denote the flow of (1) restricted to $\mathbf{F}$. For $z \in \mathbf{F}$, $X \subset \mathbf{F}$, let $d(z,X) = \inf\{\|z-a\| \mid a \in X\}$ (and so if X is compact $d(z,X)=0$ if and only if $z \in X$). If we define $\mathcal{A}_1 = \mathbf{q}_1$, then $\mathcal{A}_i \subset P_i$ is an attractor for the dynamics restricted to P_i, $i=1,2,3$. The $\mathcal{A}_i$ are connected via the sets of connections,

$$C_i = \{x \mid d(\phi_t(x), \mathcal{A}_{i+1}) \to 0 \quad \text{and} \quad d(\phi_{-t}(x), \mathcal{A}_i) \to 0 \ \text{ as } \ t \to \infty\}.$$

Equivalently, we may write

$$C_i = W^u(\mathcal{A}_i) \cap W^s(\mathcal{A}_{i+1}),$$

where $W^{u/s}$ are the unstable (resp., stable) sets of $\mathcal{A}_i$.

Provided that $\mathbf{y}^F \neq \mathbf{y}^A$, the cycle for (1) is given by

$$\Sigma = \bigcup_{i=1}^{3} \mathcal{A}_i \cup C_i.$$

We can define a connection C_i as being *phase resetting* if it is a single trajectory. In the case that C_i is nonresetting, the following question arises.

Selection of connections: Given an asymptotically stable robust cycle Σ with basin of attraction $B(\Sigma)$, what is the *likely limit set* of $B(\Sigma)$ (in the sense of Milnor[19])? In other words, if we discount sets of zero measure in the basin of $B(\Sigma)$, what subset Σ' of Σ is unavoidable for the ω-limit sets of points in $B(\Sigma)$?

This problem was raised and partially addressed in Ref. 20 for a heteroclinic cycle between equilibria. It was found that for the two-dimensional connection sets studied that if E_i was the strongly unstable eigenspace at A_i then Σ' was typically a union of one-dimensional connections (corresponding to the strong unstable manifolds) if $\dim(E_i)=1$; whereas $\Sigma'=\Sigma$ if $\dim(E_i)=2$, and the strongly unstable eigenvalues are complex.

Even for direct products of rather simple systems, the problem of cycle selection seems to be very subtle—see Ref. 21. However, it is possible to obtain results showing an absence of cycle selection if we assume strong enough results on nodal dynamics (the existence of Markov partitions). We refer to Ref. 21 for more details.

In the context of connections between chaotic sets, there is a significant new feature. Connections selected in an attractor determine the approach to the chaotic saddles and may, for example, select "atypical" routes of approach that give different Lyapunov exponents to that expected for any "natural" measure.

For model (1) in cases where the C_i are more than one dimensional, we do not understand which connections will typically be selected, and this may be a feature that is vital in understanding the dynamics near more general chaotic itinerant attractors. Even numerical simulations are not at all easy to interpret. Possibly, a better approach is to consider a noise-perturbed system in which case cycle selection will only occur on a probabilistic level.

V. DISCUSSION

In summary, we have introduced a new model system in which one can observe a variety of cycling attractors with and without phase resetting connections. Phase resetting is not possible in the system discussed in Ref. 10 because it is a global skew product. This model system is locally well approximated by a skew product near each of the nodes, but

is not globally a skew product. Although the system is carefully constructed to have the desired behavior, it should be stressed that the connections will be robust to any perturbation of the system as long as the symmetries are preserved and the nature of the chaos is not changed too greatly. In this sense, the values of the parameters and the exact forms of the functions chosen are relatively unimportant.

We believe that the property of phase resetting deserves a closer examination in more general chaotic itinerant attractors, as does the question of cycle selection, which may be helpful in a better statistical understanding of these attractors.

ACKNOWLEDGMENTS

This research was partially supported by National Science Foundation (NSF) Grant No. DMS-0071735, and by EPSRC Grants No. GR/R63530 and No. GR/N14408.

[1] W. J. Freeman and C. A. Skarda, "Spatial EEG patterns, nonlinear dynamics and perception—the neo-Sherringtonian view," Brain Res. Rev. **10**, 147–175 (1985).
[2] K. Kaneko, "On the strength of attractors in a high-dimensional system: Milnor attractor network, robust global attraction, and noise-induced selection," Physica D **124**, 308–330 (1998).
[3] J. Guckenheimer and P. Holmes, "Structurally stable heteroclinic cycles," Math. Proc. Cambridge Philos. Soc. **103**, 189–192 (1988).
[4] T. Chawanya, "Coexistence of infinitely many attractors in a simple flow," Physica D **109**, 201–241 (1997).
[5] M. Krupa, "Robust heteroclinic cycles," J. Nonlinear Sci. **7**, 129–176 (1997).
[6] D. Hansel, G. Mato, and C. Meunier, "Clustering and slow switching in globally coupled phase oscillators," Phys. Rev. E **48**, 3470–3477 (1993).
[7] H. Kori and Y. Kuramoto, "Slow switching in globally coupled oscillators: Robustness and occurrence through delayed coupling," Phys. Rev. E **63**, 046214 (2001).
[8] P. Ashwin and M. Field, "Heteroclinic networks in coupled cell systems," Arch. Ration. Mech. Anal. **148**, 107–143 (1999).
[9] M. Timme, F. Wolf, and T. Geisel, "Prevalence of unstable attractors in networks of pulse-coupled oscillators," Phys. Rev. Lett. **89**, 154105 (2002).
[10] P. Ashwin, "Cycles homoclinic to chaotic sets; robustness and resonance," Chaos **7**, 207–220 (1997).
[11] M. Dellnitz, M. Field, M. Golubitsky, A. Hohmann, and J. Ma, "Cycling chaos," IEEE Trans. Circuits Syst., I: Fundam. Theory Appl. **42**, 821–823 (1995).
[12] P. Ashwin, A. M. Rucklidge, and R. Sturman, "Infinities of periodic orbits near robust cycling," Phys. Rev. E **66**, 035201(R) (2002).
[13] P. Ashwin, A. M. Rucklidge, and R. Sturman, "Cycling attractors of coupled cell systems and dynamics with symmetry," *Proceedings of NATO ASI on Synchronization*, Crimea, May 2002 (to be published).
[14] P. Ashwin and A. M. Rucklidge, "Cycling chaos: its creation, persistence and loss of stability in a model of nonlinear magnetoconvection," Physica D **122**, 134–154 (1998).
[15] O. E. Rössler, "Continuous chaos: four prototype equations," *Bifurcation Theory and Applications*, edited by O. Gurel and O. E. Rössler, Ann. N.Y. Acad. Sci. **316**, 376–392 (1979).
[16] M. Field, *Dynamics, Bifurcation and Symmetry*, Pitman Research Notes in Mathematics (Longman, New York, 1996), Vol. 356, Chap. 6.
[17] S.-N. Chow, B. Deng, and B. Fiedler, "Homoclinic bifurcation at resonant eigenvalues," J. Diff. Eqns. **2**, 177–244 (1990).
[18] A. Pikovsky, O. Popovych, and Yu. Maistrenko, "Resolving clusters in chaotic ensembles," Phys. Rev. Lett. **87**, 044102 (2001).
[19] J. Milnor, "On the concept of attractor," Commun. Math. Phys. **99**, 177–195 (1985); **102**, 517–519 (1985).
[20] P. Ashwin and P. Chossat, "Attractors for robust heteroclinic sets with a continuum of connections," J. Nonlinear Sci. **8**, 103–129 (1997).
[21] P. Ashwin and M. Field, "Product dynamics for heteroclinic attractors," in preparation.